X-Ray Structure and Crystal Lattice Interactions of the Taxol Side-Chain Methyl Ester[1]

John R. Peterson,[2,4] Hoang D. Do,[2] and Robin D. Rogers[3]

Received December 17, 1990; accepted February 12, 1991

A colorless, parallelepiped crystal of methyl (2*R*,3*S*)-*N*-benzoyl-3-phenylisoserinate belonging to the space group $P2_1$ with a = 5.414(4), b = 7.813(1), c = 17.802(7) Å, β = 90.87(4)°, Z = 2, V = 752.9 Å^3, D_{calc} = 1.32 g cm^{-3}, and μ_{calc} = 1.02 cm^{-1} was selected and the structure solved using direct methods. Refinement led to a final R = 0.079 for 819 [$F_o \geq 5\sigma(F_o)$] reflections. Intermolecular hydrogen-bonding interactions are prevalent in the crystal lattice of this compound.

KEY WORDS: taxol side chain; crystal structure; crystal lattice interactions.

INTRODUCTION

Taxol (NSC-125973) functions as a mitotic spindle poison and as an inhibitor of *in vitro* cell replication (1–3). In striking contrast to other plant-derived antimitotics such as podophyllotoxin and colchicine, which disrupt microtubule assembly and mitotic spindle formation by reversible binding to tubulin (4), taxol promotes the assembly of microtubules upon binding to microtubule protein and stabilizes these microtubules against depolymerization. Taxol was selected for clinical development by the National Cancer Institute in 1977 based upon its unique mechanism of action and its strong activity against the B16 melanoma and the MX-1 human mammary xenograft. The drug has since progressed through Phase I clinical trials, but Phase II investigations of taxol have been severely hindered by inadequate drug supply in spite of promising activity against melanoma and ovarian cancer. Taxol is presently obtained in extremely low yield (0.004–0.016%) from the bark of the western yew, *Taxus brevifolia* (5). Synthetic efforts toward taxol have been hampered by its structural and stereochemical complexity. An efficient, enantioselective synthesis of the taxol side chain was reported by Greene and co-workers (6,7). The coupling of this side chain to naturally procured 10-deacetyl baccatin III is the most promising strategy to taxol to date (8).

In conjunction with a study focused on the design and discovery of new substances that mimic taxol in its mechanism of action (9), we now report the X-ray structure and crystal lattice interactions of methyl (2*R*,3*S*)-(−)-*N*-benzoyl-3-phenylisoserinate, the taxol side-chain methyl ester. The *N*-benzoyl-3-phenylisoserine ester at position 13 of the taxol A-ring is required for potent antimitotic activity (1–3). In contrast, cephalomannine, which differs from taxol only in side-chain substitution, exhibits substantially diminished activity (3). We project that a detailed understanding of the molecular features of the taxol side chain may facilitate the intelligent design of new analogs and taxol mimics. An X-ray analysis of the taxol side-chain 4-bromobenzoate was accomplished earlier, although the details of this structure analysis were not reported (5). A crystal structure of the cephalomannine side-chain methyl ester was reported by Clardy and co-workers (10) (Scheme I).

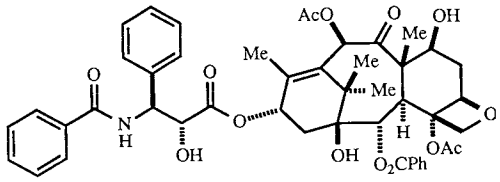

Scheme I. Taxol.

MATERIALS AND METHODS

The taxol side-chain methyl ester [methyl (2*R*,3*S*)-(−)-*N*-benzoyl-3-phenylisoserinate] was prepared by a literature procedure (6,7). The X-ray structural data were collected on an Enraf-Nonius CAD-4 diffractometer with graphite monochromator and MoKα (λ = 0.71073 Å) radiation. NMR spectra were accumulated at 300 MHz for hydrogen and at 75 MHz for carbon on a Varian VXR 300 instrument. The infrared spectrum was obtained on a Perkin–Elmer 281B infrared spectrophotometer. The melting point was determined in an open capillary tube with a Thomas–Hoover capillary melting-point apparatus and the optical rotation measured on a JASCO DIP-370 digital polarimeter.

Physical Data of Methyl (2R,3S)-(−)-N-Benzoyl-3-Phenyl isoserinate (6). mp 183–184°C ($CHCl_3$), lit. mp 184–185°C ($CHCl_3$); $[\alpha]^{25}_D$ −45.1° (MeOH), lit. $[\alpha]^{26}_D$ −48° (MeOH); IR (KBr) 3360 (br), 3030, 2980, 2940, 1730, 1640, 1600, 1580, 1545, 1520, 1480, 1435, 1410, 1365, 1320, 1290, 1260, 1200, 1180, 1155, 1120, 1110, 1055, 1025, 980, 930, 875, 840, 800, 760, 720, 705, 610 cm^{-1}; ^{1}H NMR ($CDCl_3$) δ 7.79–7.75 (m, 2 H), 7.54–7.27 (m, 8 H), 7.02 (d, J = 8.93 Hz, 1 H), 5.75 (dd, J = 8.93, 2.00 Hz, 1 H), 4.64 (d, J = 2.00 Hz, 1 H), 3.84 (s, 3 H), 3.39 (br s, 1 H); ^{13}C NMR[5] ($CDCl_3$) δ 173.3 (0), 166.8 (0), 138.6 (0), 134.0 (0), 131.7 (1), 128.7 (1), 128.6 (1), 127.9 (1), 127.0 (1), 126.8 (1), 73.2 (1), 54.8 (1), 53.2 (3).

[1] Supplementary material available from the authors: Table SI. Final Fractional Coordinates for H Atoms of $C_{17}H_{17}NO_4$; Table SII. Thermal Parameters for $C_{17}H_{17}NO_4$; Table SIII. Least-Squares Planes for $C_{17}H_{17}NO_4$; Table SIV. Observed and Calculated Structure Factors for $C_{17}H_{17}NO_4$.

[2] Department of Pharmacognosy and the Research Institute of Pharmaceutical Sciences, School of Pharmacy, The University of Mississippi, University, Mississippi 38677.

[3] Department of Chemistry, Northern Illinois University, DeKalb, Illinois 60115.

[4] To whom correspondence should be addressed.

[5] Numbers in parentheses for the ^{13}C NMR data indicate the number of attached hydrogens on that carbon as determined by the attached proton test (ATP).

0724-8741/91/0700-0908$06.50/0

Table I. Final Fractional Coordinates for $C_{17}H_{17}NO_4$

Atom	x/a	y/b	z/c	B(eqv)[a]
O(1)	−0.515 (2)	−0.393 (2)	−0.2652 (6)	4.91
O(2)	−0.137 (2)	−0.399 (2)	−0.2161 (5)	3.31
O(3)	−0.669 (1)	−0.168 (2)	−0.1618 (4)	2.89
O(4)	0.084 (1)	0.020 (2)	−0.2967 (4)	3.42
N	−0.311 (1)	0.0000	−0.2652 (5)	1.96
C(1)	−0.373 (2)	−0.344 (2)	−0.2203 (7)	2.65
C(2)	−0.415 (2)	−0.198 (2)	−0.1677 (6)	2.25
C(3)	−0.276 (2)	−0.040 (2)	−0.1904 (7)	2.38
C(4)	−0.311 (2)	0.112 (2)	−0.1346 (6)	2.37
C(5)	−0.165 (3)	0.137 (2)	−0.0776 (8)	3.54
C(6)	−0.188 (3)	0.267 (2)	−0.0236 (9)	4.71
C(7)	−0.404 (3)	0.377 (2)	−0.0372 (8)	3.38
C(8)	−0.558 (3)	0.350 (2)	−0.0963 (9)	3.76
C(9)	−0.522 (2)	0.215 (2)	−0.1465 (7)	3.08
C(10)	−0.123 (2)	0.023 (2)	−0.3144 (7)	2.30
C(11)	−0.198 (2)	0.042 (2)	−0.3967 (6)	2.06
C(12)	−0.023 (2)	0.131 (2)	−0.4396 (7)	2.92
C(13)	−0.090 (2)	0.145 (2)	−0.5196 (8)	3.40
C(14)	−0.284 (3)	0.067 (2)	−0.5486 (7)	3.71
C(15)	−0.452 (2)	−0.023 (2)	−0.5054 (8)	3.38
C(16)	−0.406 (2)	−0.032 (2)	−0.4284 (7)	2.70
C(17)	−0.083 (3)	−0.541 (2)	−0.2691 (9)	5.07

[a] $B(\text{eqv}) = 4/3[a^2\beta_{11} + b^2\beta_{22} + c^2\beta_{33} + ab(\cos\gamma)\beta_{12} + ac(\cos\beta)\beta_{13} + bc(\cos\alpha)\beta_{23}]$.

Crystal Data, Structure Determination, and Refinement. A colorless, parellelepiped crystal of $C_{17}H_{17}NO_4$, molecular weight 299.33, with dimensions 0.10 × 0.23 × 0.40 mm was selected, mounted on a pin, and transferred to the goniometer. The space group was determined to be either the centric $P2_1/m$ or the acentric $P2_1$ from the systematic absences. Statistical tests indicated that the space was acentric and the subsequent solution and successful refinement of the structure was carried out in the acentric space group $P2_1$. Cell constants were obtained from the setting angles of 25 reflections ($\theta > 16°$). Unit cell dimensions were $a = 5.414(4)$, $b = 7.813(1)$, and $c = 17.802(7)$ Å, $\beta = 90.87(4)°$, $V = 752.9$ Å^3, $Z = 2$, $D_{calc} = 1.32$ g cm^{-3}, and $\mu_{calc} = 1.02$ cm^{-1}. A total of 1581 reflections was measured; 819 were considered observed [$F_o \geq 5\sigma(F_o)$] reflections and included in the refinement. The intensities were corrected for Lorentz-polarization effects. Index range: h 0 to 6, k 0 to 9, l −21 to 21 for $2\theta \geq 50°$. The structure was solved using the SHELXS (11) direct methods program. The geometrically constrained hydrogen atoms were placed in calculated positions 0.95 Å from the bonded carbon atom and allowed to ride on that atom with B fixed at 5.5 Å^2. The methyl hydrogen atoms were included as a rigid group with rotational freedom at the bonded carbon atom (C–H = 0.95 Å, B = 5.5 Å^2). The remaining hydrogen atoms were located from a difference Fourier map and included with fixed contributions (B = 5.5

Table II. Bond Distances (Å) and Angles (deg) for $C_{17}H_{17}NO_4$

Atoms	Distance	Atoms	Distance
O(1)–C(1)	1.17 (1)	O(2)–C(1)	1.35 (1)
O(2)–C(17)	1.49 (2)	O(3)–C(2)	1.40 (1)
O(4)–C(10)	1.16 (1)	N–C(3)	1.38 (1)
N–C(10)	1.37 (1)	C(1)–C(2)	1.50 (2)
C(2)–C(3)	1.51 (2)	C(3)–C(4)	1.56 (2)
C(4)–C(5)	1.29 (2)	C(4)–C(9)	1.41 (2)
C(5)–C(6)	1.40 (2)	C(6)–C(7)	1.47 (2)
C(7)–C(8)	1.35 (2)	C(8)–C(9)	1.40 (2)
C(10)–C(11)	1.52 (2)	C(11)–C(12)	1.41 (2)
C(11)–C(16)	1.38 (2)	C(12)–C(13)	1.47 (2)
C(13)–C(14)	1.31 (2)	C(14)–C(15)	1.39 (2)
C(15)–C(16)	1.39 (2)		
Atoms	**Angle**	**Atoms**	**Angle**
C(1)–O(2)–C(17)	114 (1)	C(3)–N–C(10)	123.8 (9)
O(1)–C(1)–O(2)	123 (1)	O(1)–C(1)–C(2)	125 (1)
O(2)–C(1)–C(2)	111 (1)	O(3)–C(2)–C(1)	110 (1)
O(3)–C(2)–C(3)	112 (1)	C(1)–C(2)–C(3)	112.2 (9)
N–C(3)–C(2)	112 (1)	N–C(3)–C(4)	115 (1)
C(2)–C(3)–C(4)	112.8 (8)	C(3)–C(4)–C(5)	122 (1)
C(3)–C(4)–C(9)	116 (1)	C(5)–C(4)–C(9)	121 (1)
C(4)–C(5)–C(6)	126 (2)	C(5)–C(6)–C(7)	113 (2)
C(6)–C(7)–C(8)	121 (1)	C(7)–C(8)–C(9)	122 (2)
C(4)–C(9)–C(8)	117 (1)	O(4)–C(10)–N	123 (1)
O(4)–C(10)–C(11)	120 (1)	N–C(10)–C(11)	116.1 (9)
C(10)–C(11)–C(12)	113 (1)	C(10)–C(11)–C(16)	124 (1)
C(12)–C(11)–C(16)	122 (1)	C(11)–C(12)–C(13)	114 (1)
C(12)–C(13)–C(14)	122 (1)	C(13)–C(14)–C(15)	123 (1)
C(14)–C(15)–C(16)	117 (1)	C(11)–C(16)–C(15)	121 (1)

Å^2). The mosaic spread in all of the crystals studied (five) was quite large. It is quite likely that this is the cause of the high R values obtained in this study. Scattering factors and anomalous-dispersion corrections were from the *International Tables for X-Ray Crystallography* (12). The structure was refined with SHELX76 (13). $\Sigma\, w(|F_o| - |F_c|)^2$ was minimized and 201 parameters were varied during the final refinement. Weights = $[\sigma(F_o)^2 + 0.00065\, F_o^2]^{-1}$, final R = 0.079, R_w = 0.102, $R_{\text{inverse configuration}}$ = 0.079, S = 5.78. Δ/σ in the final least-squares refinement cycle <0.01, $\Delta\rho$ < 0.6 e^- Å^{-3} in the final difference map. The final fractional coordinates for the taxol side-chain methyl ester are listed in Table I.

RESULTS AND DISCUSSION

The derived bond distances and angles and the torsion angles for the taxol side chain methyl ester are provided in Tables II and III, respectively. An ORTEP diagram (14) is illustrated in Fig. 1 and a cell plot for this compound in Fig. 2.

The aromatic ring atoms C(4) through C(9) and C(11) through C(16) define unique planes to within 0.018 and 0.033 Å, respectively. Atom C(3) deviates from the former plane by 0.032 Å and carbonyl carbon C(10) from the C(11)–C(16) plane by −0.099 Å. The amide plane, defined by atoms O(4), C(10), C(11), and N, intersects the C(11)–C(16) aromatic ring plane at an angle of 29.1°. The carbonyl atoms O(1), C(1), O(2), and C(2) are in turn planar to within 0.041 Å, and the methoxy atoms O(3) and C(17), respectively, deviate from this plane by 0.322 and −0.009 Å. The carbomethoxy and phenyl groups on atoms C(2) and C(3) adopt a nearly *anti* relationship with respect to each other as evidenced by the C(1)—C(2)—C(3)—C(4) torsion angle of −178.0° and the H(1)C(2)—C(2)—C(3)—H(1)C(3) torsion angle of 54.9°. Likewise, the H(1)C(3)—C(3)—N—C(10) torsion angle of −10.2° indicates that the amide carbonyl and H(1)C(3) are almost eclipsed. Bond distances and angles about the isoserinate chain are close to values normally associated with sp^2- and sp^3-hybridized carbon centers. The carbonyl distances O(1)—C(1) and O(4)—C(10) are 1.17(1) and 1.16(1) Å, respectively, the C(1)—C(2) bond length is 1.50(2) Å, the C(2)—C(3) distance is 1.51(2) Å, and the C(3)—C(4) separation is 1.56(2) Å. The minor bond distance fluctuations in the aromatic rings are most likely a crystallographic artifact, resulting from the low quality of the data available.

Table III. Torsion Angles (deg) for $C_{17}H_{17}NO_4$

Atoms	Angle
C(1)–C(2)–C(3)–C(4)	−178.0
O(3)–C(2)–C(3)–C(4)	58.2
H(1)C(2)–C(2)–C(3)–C(4)	−57.3
C(1)–C(2)–C(3)–N	49.4
O(3)–C(2)–C(3)–N	−74.3
H(1)C(2)–C(2)–C(3)–N	170.1
C(1)–C(2)–C(3)–H(1)C(3)	−65.8
O(3)–C(2)–C(3)–H(1)C(3)	170.5
H(1)C(2)–C(2)–C(3)–H(1)C(3)	54.9
C(2)–C(3)–N–C(10)	−125.8
C(2)–C(3)–N–H(1)N	38.7
C(4)–C(3)–N–C(10)	102.9
C(4)–C(3)–N–H(1)N	−92.5
H(1)C(3)–C(3)–N–C(10)	−10.2
H(1)C(3)–C(3)–N–H(1)N	154.3

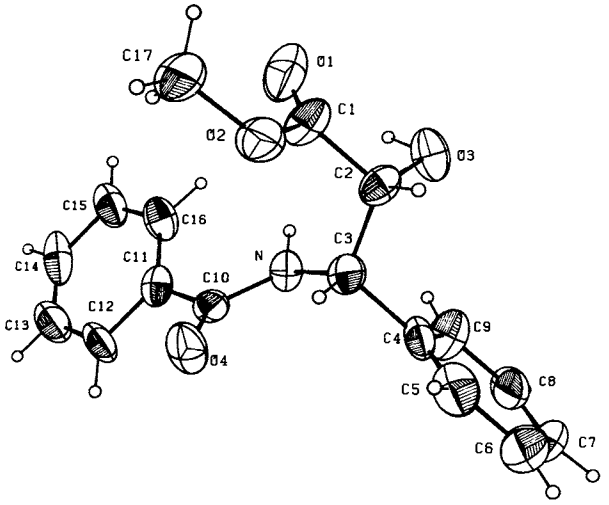

Fig. 1. Thermal-ellipsoid plot of the taxol side-chain methyl ester illustrating the atom-numbering scheme. The hydrogen atom radii are arbitrarily reduced.

An analysis of contact distances reveals that hydrogen bonds and van der Waals interactions are the dominant stabilizing forces in the crystal lattice of the title compound. Notable intermolecular contact distances of less than 3.5 Å are tabulated in Table IV. The hydrogen-bonding interactions for the taxol side-chain methyl ester form polymeric chains along a and are illustrated in Fig. 3. Specifically, hydrogen bonds exist between atoms O(4) ··· H(1)O(3) and O(4) ··· H(1)N with internuclear separations of 2.23 and 2.35 Å, respectively, for a molecule at $x + 1, y, z$ relative to the reference molecule at x, y, z. The O(3)–H(1)O(3) ··· O(4) and the N–H(1)N ··· O(4) angles are 138 and 150°, respectively.

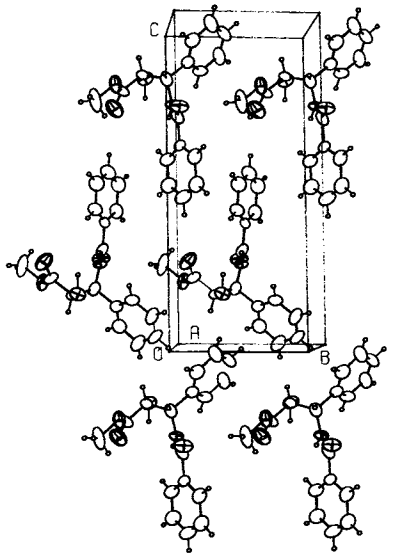

Fig. 2. Cell plot of the title compound.

Table IV. Intermolecular Contacts (Å) for the Taxol Side-Chain Methyl Ester

Atoms	Distance		Atoms	Distance	
O(2)···H(1)O(3)	2.81	I	O(2)···O(3)	3.25 (1)	I
O(2)···O(1)	3.49 (1)	I	O(4)···H(1)O(3)	2.23	I
O(4)···O(3)	3.10 (1)	I	O(4)···H(1)N	2.35	I
O(4)···N	3.32 (1)	I	O(4)···H(1)C(9)	2.80	I
O(4)···H(1)C(16)	2.93	I	H(1)C(3)···H(1)O(3)	2.21	I
H(1)C(3)···O(3)	2.52	I	C(3)···O(3)	3.46 (1)	I
H(1)C(12)···H(1)C(16)	2.88	I	H(1)C(17)···O(1)	2.63	I
C(17)···O(1)	3.28 (2)	I			
N···H(2)C(17)	2.92	II	C(8)···C(1)	3.41 (2)	II
C(10)···H(2)C(17)	2.82	II			
H(1)C(2)···H(1)C(6)	2.94	III	H(1)C(5)···H(1)C(7)	2.93	III
H(1)C(5)···H(1)C(6)	2.41	III			
H(1)C(17)···H(1)C(9)	2.77	IV			
H(1)C(6)···O(3)	2.97	V	C(6)···O(3)	3.44 (2)	V
H(1)C(7)···H(1)C(2)	2.87	V	H(1)C(7)···C(5)	2.92	V
O(1)···H(1)C(14)	2.55	VI	O(1)···C(14)	3.49 (2)	VI
H(1)C(15)···C(13)	2.89	VI	H(1)C(16)···H(1)C(14)	2.77	VI
H(1)C(13)···H(3)C(17)	2.86	VII	H(1)C(13)···C(11)	2.94	VII
H(1)C(13)···C(16)	2.96	VII	H(1)C(14)···H(3)C(17)	2.84	VII
H(1)C(14)···H(1)C(17)	2.91	VII			

Roman numerals denote the following positions relative to the reference molecule at x, y, z:

I	$x + 1, y, z$
II	$x, y + 1, z$
III	$-x, y - 1/2, -z$
IV	$x + 1, y - 1, z$
V	$-1 - x, 1/2 + y, -z$
VI	$-1 - x, y - 1/2, -1 - z$
VII	$-x, 1/2 + y, -1 - z$

The H(1)O(3) ··· O(4) ··· H(1)N angle is 60°. Particularly short van der Waals contacts include H(1)C(3) ··· H(1)O(3) of 2.21 Å and H(1)C(3) ··· O(3) of 2.52 Å for a molecule at $x + 1, y, z$, H(1)C(5) ··· H(1)C(6) of 2.41 Å for a molecular at $-x, y - 1/2, -z$, and O(1) ··· H(1)C(14) of 2.55 Å for a molecule at $-1 - x, y - 1/2, -1 - z$, all of which are relative to the reference molecule at x, y, z.

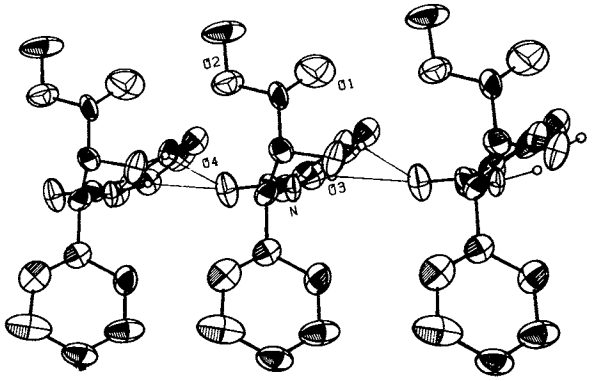

Fig. 3. Intermolecular hydrogen-bond interactions of the title compound.

In conclusion, the crystal structure of methyl (2*R*,3*S*)-(−)-*N*-benzoyl-3-phenylisoserinate, the taxol side-chain methyl ester, was solved for the first time by the use of direct methods. Several prominent intermolecular hydrogen bonds and van der Waals contacts occur in the crystal lattice of this compound. We speculate that such interactions could be important in the binding of taxol or potential taxol mimics to the microtubule protein receptor site. Extensive chemical, structural, and biological investigations of molecules designed to mimic taxol, and which incorporate a (2*R*,3*S*)-(−)-*N*-benzoyl-3-phenylisoserinate side chain, are now in progress in our laboratories.

ACKNOWLEDGMENTS

The authors are indebted to the Milheim Foundation for Cancer Research (Grant 89-21; J.R.P.) and the Elsa U. Pardee Foundation (J.R.P.) for their generous support of this research. The U.S. National Science Foundation Chemical Instrumentation Program provided funding to purchase the diffractometer (R.D.R.).

REFERENCES

1. M. Suffness. Development of antitumor natural products at the National Cancer Institute. *Gann Monogr. Cancer Res.* **36**:21–44 (1989).
2. M. Suffness and G. A. Cordell. Antitumor alkaloids. In A. Brossi (ed.), *The Alkaloids, Chemistry and Pharmacology,* Academic Press, Orlando, FL, 1985, Vol. XXV, pp. 1–18, 280–288.
3. D. G. I. Kingston, G. Samaranayake, and C. A. Levy. The chemistry of taxol, a clinically useful anticancer agent. *J. Nat. Prod.* **53**:1–12 (1990).
4. I. Jardine. Podophyllotoxins. In J. M. Cassady and J. D. Douros (eds.), *Anticancer Agents Based on Natural Product Models,* Academic Press, New York, 1980, pp. 319–351.
5. M. C. Wani, H. L. Taylor, M. E. Wall, P. Coggon, and A. T. McPhail. Plant antitumor agents. VI. The isolation and structure of taxol, a novel antileukemic and antitumor agent from *Taxus brevifolia. J. Am. Chem. Soc.* **93**:2325–2327 (1971).
6. J.-N. Denis, A. E. Greene, A. A. Serra, and M.-J. Luche. An efficient, enantioselective synthesis of the taxol side chain. *J. Org. Chem.* **51**:46–50 (1986).
7. J.-N. Denis, A. Correa, and A. E. Greene. An improved synthesis of the taxol side chain and of RP 56976. *J. Org. Chem.* **55**:1957–1959 (1990).
8. J.-N. Denis, A. E. Greene, D. Guénard, F. Guéritte-Voegelein, L. Mangatal, and P. Potier. A highly efficient, practical approach to natural taxol. *J. Am. Chem. Soc.* **110**:5917–5919 (1988).
9. H. D. Do. *The Synthesis and Biological Activity of Podophyllotoxin and Taxol Analogs,* Ph.D. thesis, Northern Illinois University, DeKalb, 1990.
10. R. W. Miller, R. G. Powell, C. R. Smith, Jr., E. Arnold, and J. Clardy. Antileukemic alkaloids from *Taxus wallichiana* Zucc. *J. Org. Chem.* **46**:1469–1474 (1981).
11. G. M. Sheldrick. *SHELXS.* In G. M. Sheldrick, C. Krüger, and R. Goddard (eds.), *Crystallographic Computing 3,* University Press, Oxford, England 1985, pp. 175–189.
12. *International Tables for X-Ray Crystallography, Vol IV,* Kynoch Press, Birmingham, England, 1974, pp. 72, 99, 149. (Present distributor: Kluwer Academic Publishers, Dordrect.)
13. G. M. Sheldrick. *SHELX76,* a system of computer programs for X-ray structure determination as locally modified, University of Cambridge, England, 1976.
14. C. K. Johnson. *ORTEP II,* Report on ORNL-5138, Oak Ridge National Laboratory, Oak Ridge, TN, 1976.